High-temperature Spectrophotometric and Electron Spin Resonance Spectroscopic Investigations of Vanadium Complexes in the Molten Salt–Gas System V_2O_5–$K_2S_2O_7$/SO_2–SO_3–N_2†

Dimitris A. Karydis,[a] Kim M. Eriksen,[b] Rasmus Fehrmann[b] and Soghomon Boghosian*[,a]

[a] *Institute of Chemical Engineering and High Temperature Chemical Processes (ICE/HT-FORTH), Department of Chemical Engineering, University of Patras, GR-26500 Patras, Greece*

[b] *Chemistry Department A, The Technical University of Denmark, DK-2800 Lyngby, Denmark*

Electronic absorption (UV/VIS) and ESR spectra have been obtained in the temperature ranges 430–480 °C and 355–478 °C from V_2O_5–$K_2S_2O_7$ molten mixtures in the composition range 0.1–0.5 mol dm^{-3} V_2O_5 in contact with SO_2 and SO_3 (P_{SO_2}/P_{SO_2} = 0.1–5, $P_{SO_2} + P_{SO_3}$ = 0.1 atm, $P_{N_2} \approx 0.9$ atm). The data obtained by both spectrophotometric and ESR methods indicate that the interaction of SO_2 and SO_3 with the melts results in a redox equilibrium between monomeric or dimeric V^V and monomeric V^{IV} complexes. An absorption band centred at 730 nm due to the V^{IV} complexes was observed and the molar absorption coefficients at 730 nm due to the V^{IV} and V^V complexes (tail of V^V charge transfer band) were found to be $\varepsilon_{V^{IV},730} = 18.91 \pm 0.08$ and $\varepsilon_{V^V,730} = -2.7 + 9.48 \times 10^{-3}\,T$ $dm^3\ mol^{-1}\ cm^{-1}$ in the temperature range $430 < T < 480$ °C. The characteristic eight-line feature of the ESR spectra with $g = 1.979 \pm 0.005$ and $\bar{A} = 111 \pm 5$ G confirms the presence of V^{IV} in monomeric complexes, presumably $[VO(SO_4)_2]^{2-}$, in the melts. From the temperature-dependence studies of the electronic absorption spectra the equilibrium constants and enthalpies for a number of possible equilibria have been calculated.

It is well established that molten mixtures of vanadium pentaoxide and alkali disulfates catalyse the oxidation of SO_2 by O_2 to SO_3. These mixtures are considered as realistic models of the active part of the sulfuric acid catalyst. In the industrial process of sulfuric acid production, oxidation of SO_2 occurs as a homogeneous reaction in the liquid phase, which is dispersed on an inert support. Since the first report[1] of a suggested two-step reaction mechanism involving a vanadium reduction step ($V^V \longrightarrow V^{IV}$), no definite conclusion has been made for the SO_2 oxidation mechanism on a molecular level. Under certain conditions reaction paths not involving tetravalent vanadium have also been proposed[2] making the overall picture more complicated. The only common features supported by numerous investigations dealing with two-, three- or multi-step reaction paths[3] appear to be: (*a*) establishment of a fast equilibrium by the interaction of SO_2 with a V^V species and (*b*) a slow (rate-determining) interaction of oxygen with a catalyst component restoring the catalytically active V^V complex. Nevertheless, the nature of the catalytically important vanadium species is still uncertain.

Direct spectroscopic study of the supported liquid catalyst is often impossible. However, further insight into the chemistry of the catalyst may be gained by investigating the molten salt–gas system V_2O_5–$M_2S_2O_7$/SO_2–SO_3–O_2–N_2 (M = K, Na, Cs or mixtures of these), which is a realistic model of the working catalyst. So far thermal, electrochemical and spectroscopic methods have been applied giving some information about V^V complex formation in model melts.[4–7] Furthermore, the phase diagrams of the catalytically important V_2O_5–$M_2S_2O_7$ (M = 80% K + 20% Na),[8] V_2O_5–$K_2S_2O_7$[9] and V_2O_5–$Cs_2S_2O_7$[10] systems have been constructed. Precipitation of tetravalent and trivalent crystalline vanadium compounds [namely $K_4(VO)_3(SO_4)_5$, $Na_2VO(SO_4)_2$, $Cs_2(VO)_2(SO_4)_3$, $KV(SO_4)_2$, $NaV(SO_4)_2$ and $CsV(SO_4)_2$] has been shown to cause deactivation of catalyst model melts during SO_2 oxidation.[11] Structural characterization of these compounds has been performed by X-ray diffraction and spectroscopic methods.[12–16] Formation of $K_4(VO)_3(SO_4)_5$ was also confirmed in a working industrial catalyst by *in situ* ESR measurements.[17]

In the present work, for the first time high temperature UV/VIS and ESR spectroscopic methods are applied to study the complex formation of V^{IV} in the molten salt–gas system V_2O_5–$K_2S_2O_7$/SO_2–SO_3–N_2. An optical furnace and a high temperature ESR cavity have been coupled to a catalyst-test apparatus to enable the comprehensive study of the redox equilibrium involving V^{IV} and V^V complexes under various partial pressures of SO_2 and SO_3. Previously, only an electrochemical investigation[18] of V^{IV} complexes in molten $K_2S_2O_7$ had been carried out, where the V^{IV} species $VOSO_4$ and $VO(SO_4)_3^{4-}$ were claimed to exist in the melt. However, these results are considered doubtful since the experimental conditions, as explained before in ref. 12, were not well defined (*e.g.* use of 'wet' chemicals, unknown partial pressure of SO_2).

This investigation is concerned only with more simple dilute solutions of V^{IV}, *i.e.* below 1 mol dm^{-3}, which is lower than the vanadium concentration of 3–6 mol dm^{-3} in industrial catalysts. This is because the highly concentrated catalyst-model melts seem to contain a very complicated mixture of partly polymerized V^{IV} complexes, as judged from earlier ESR measurements on working catalysts.[17,19] A future publication will deal with these solutions.

Experimental

Materials.—The $K_2S_2O_7$ used was synthesised by thermal decomposition of $K_2S_2O_8$ (Merck, pro analysi).[4] The non-

† *Supplementary data available* (No. SUP 57016, 2 pp.): calculated molar absorption coefficients and variances for the four applied models at measured temperatures. See Instructions for Authors, *J. Chem. Soc., Dalton Trans.*, 1994, Issue 1, pp. xxiii–xxviii.

Non-SI units employed: atm = 101 325 Pa; G = 10^{-4} T.

hygroscopic V_2O_5 (Cerac, Pure 99.9%) was used without further purification. All handling of chemicals including the filling of the UV/VIS and ESR reactor cells took place in a nitrogen-filled glove-box with a measured water-vapour content of about 1–5 ppm achieved by continuous circulation of the box gas through external gas purifiers. To avoid formation of hydrogen sulfate, $K_2S_2O_7$ was kept in sealed ampoules until used, and only briefly exposed to the dry atmosphere of the glove-box. The gases used were SO_2 (Matheson, Union-Carbide 99.98% anhydrous), N_2 (L'Air Liquide, 99.999%) and O_2 (L'Air Liquide, 99.99%).

UV/VIS Spectrophotometry.—The flow diagram (Fig. 1) of the equipment used for bringing together gaseous reactants with molten-salt catalysts was modified compared to that described earlier.[11] The gas-mixing unit had four Brooks (model 5850) mass flow controllers. The nitrogen and oxygen streams were passed through gas purifiers (molecular sieves and activated charcoal traps) before entering the mass-flow controllers.

The gas mixture could then be fed to a preconverter whereby any desired SO_2–SO_3–N_2 gas mixture could be obtained by adjusting the flow of O_2, which was the limiting reactant in the gas stream entering the preconverter. The preconverter exit gas, an SO_2–SO_3–N_2 mixture containing a very small amount of O_2, *i.e.* below 0.1 mole %, entered the reactor through stainless steel and Viton rubber tubing which was electrically heated to 80–90 °C to avoid SO_3 condensation. A description of the preconverter has been given in detail elsewhere.[11] The optical gas–molten salt reactor cell shown in Fig. 2 was mounted in an upright position inside the optical furnace, which was placed in the sample compartment of a Hitachi 220S spectrophotometer. Two independent heating coils were used for heating the furnace and adjusting the temperature gradient along the optical cell by compensating for the temperature drop at the furnace windows. Rectangular fused-silica cells (Ultrasil from Helma, Germany) with 0.05, 0.2, 0.5 and 1 cm path lengths were used.

The gas was passed through the inlet joint (Fig. 2, A), downwards along the capillary tube (B) and bubbled through the optical part containing the molten mixture (C). In this way

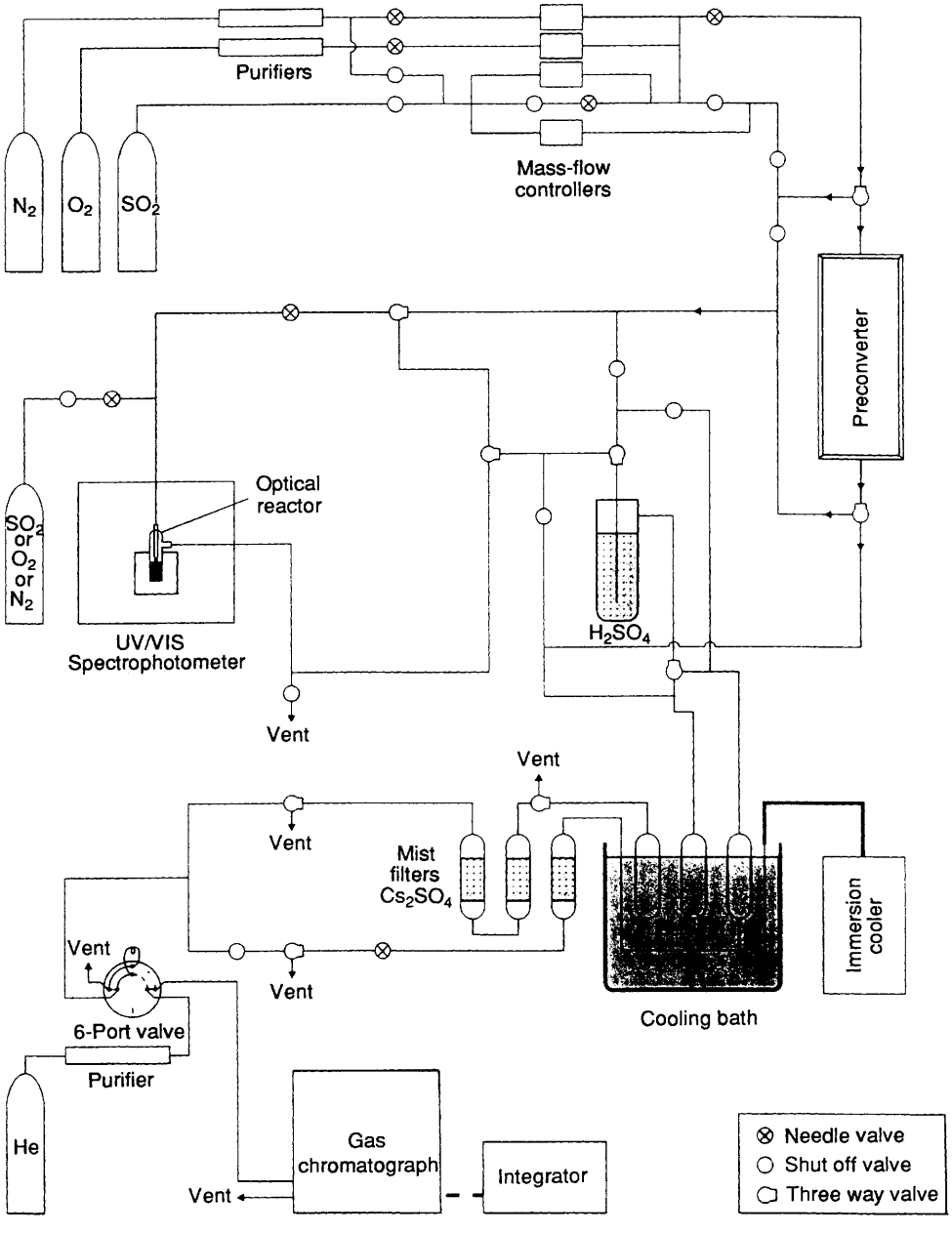

Fig. 1 Flow diagram of the experimental set-up

a very effective mixing and shortening of the time needed to reach equilibrium was achieved. The reactor exit gas was then sent through an SO_3 absorber containing H_2SO_4 (95–99%) and then to a SO_3 cold trap located inside an antifreeze bath at −35 °C. Finally the gas stream was passed through Cs_2SO_4 mist filters before flowing through the sample loop of the Shimadzu GC-9A gas chromatograph, with a thermal conductivity detector, a stainless steel column packed with Porapak Q (80–100 mesh) and equipped with a pneumatic Valco 6-port external sampling valve possessing a 2 cm^3 loop. The temperature of the preconverter was equal to the temperature of the optical reactor. In this way, the SO_2–SO_3–O_2–N_2 mixture was pre-equilibrated at the same temperature as that of the V_2O_5–$K_2S_2O_7$ molten-salt–catalyst mixture. Thus, the gas composition did not change in the optical cell as confirmed also by analysing separately the preconverter exit gas and the reactor exit gas. This could be achieved by switching the appropriate valves as shown in Fig. 1 and using the two independent flow lines interfacing with the gas chromatograph. Using this set-up simultaneous analysis of the gas and melt composition was possible.

Equilibrium in the melt was established after 3–5 h. For measuring the absorbance, the capillary (B in Fig. 2) was lifted above the melt to stop agitation. After measuring the absorbance, the gas composition was changed by regulating the O_2 flow by means of the appropriate mass-flow controller. A new value of P_{SO_2}/P_{SO_3} was then established in the gas entering the optical reactor cell.

The interpretation of the spectrophotometric measurements is based on Beer's law. If only one V^V and one V^{IV} species are present then the measured optical density, A (absorbance), is related to the concentration of the absorbing species according to equation (1) where l is the path length, $c_{V^{IV}}$ and c_{V^V} are

$$A/l = \varepsilon_{V^{IV}}c_{V^{IV}} + \varepsilon_{V^V}c_{V^V} \quad (1)$$

the equilibrium concentrations of the tetravalent and pentavalent vanadium complex species participating in the reaction expressed in moles of vanadium per dm^3, $\varepsilon_{V^{IV}}$ and ε_{V^V} are the respective absorption coefficients per mole of vanadium of the absorbing species and $c_{V^{IV}} + c_{V^V} = c_0$ [c_0 denotes the initial concentration of vanadium (based on the weighed-in amount of V_2O_5) expressed in mol dm^{-3}]. Density values for the molten V_2O_5–$K_2S_2O_7$ mixtures were taken from ref. 6 and the volume of the melt was assumed to be unchanged, regardless of any gas atmosphere applied.

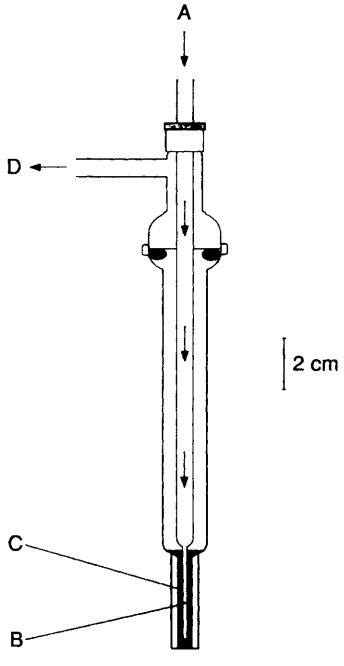

Fig. 2 Gas–molten salt optical reactor cell: A, gas inlet; B, capillary tube immersed in the melt; C, molten salt mixture, D, gas outlet. The capillary tube is lifted above the melt surface during the measurement of the spectra

ESR Spectroscopy.—An apparatus similar to the one described above was used. This was coupled with a slightly modified JEOL JES-ME-1X electron-spin resonance spectrometer equipped with a Bruker ER4114HT high-temperature cavity and a PC-based data acquisition system. The set-up consisted essentially of a preconverter for preconversion of the feed gas, an acid absorber for removal of SO_3 and a gas chromatograph. Due to insufficient stability of the mass-flow controllers in the low flow range (*ca.* 1 cm^3 min^{-1}) the feed gas was premixed in a bottle. The molten mixtures to be investigated were premixed in Pyrex ampoules under an oxygen atmosphere at 450 °C, before being loaded into the ESR reactor cell. Field calibration was performed by means of a Mn^{II} standard. Details of the experimental set-up and the ESR reactor cell have been reported previously.[17]

Results and Discussion

Spectrophotometric Measurements.—The UV/VIS spectra in the range 550–900 nm were recorded at 450 °C for 0.1 mol dm^{-3} V_2O_5 (*i.e.* 0.2 mol dm^{-3} V) solutions in $K_2S_2O_7$ under 22 different SO_2–SO_3–N_2 gaseous mixtures at a total pressure of 1 atm and in the partial pressure range P_{SO_2}/P_{SO_3} = 0.1–5, $P_{SO_2} + P_{SO_3}$ = 0.1 atm.

Molar absorption coefficients of V^{IV} *and* V^V *complexes.* Several experiments were performed for the determination of the molar absorption coefficients of V^{IV} and V^V complexes. Thus, spectra were obtained under atmospheres of SO_2 (*i.e.* P_{SO_2} = 1 atm) or O_2 and/or SO_3.

For convenience only a few spectra are shown in Fig. 3. Spectrum (*a*) (P_{SO_2} = 1 atm) shows an absorption band with a maximum around 730 nm (13 700 cm^{-1}). Here vanadium is considered completely reduced to a V^{IV} complex, since a spectrum obtained after raising P_{SO_2} to 2 atm did not show significant increase in the absorption coefficient. Presumably, according to the Balhausen–Gray scheme,[20] the vanadyl ion (VO^{2+}) is found as the central unit co-ordinated to equatorial ligands in C_{4v} symmetry. This is supported by the similarity of the spectrum to the spectra of many other vanadyl compounds[21] and from the ESR spectra (see below). In general,[21] vanadyl complexes display weak absorption bands due to the Laporte-forbidden d–d transitions $^2B_2(d_{xy}) \longrightarrow$

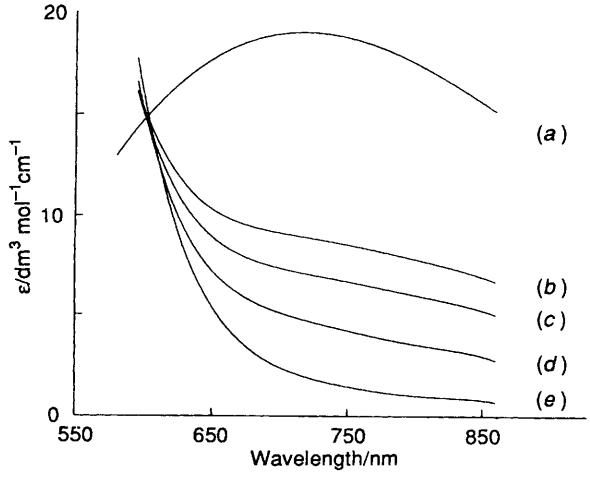

Fig. 3 VIS/NIR spectra of the V_2O_5–$K_2S_2O_7$ mixtures (c_0 = 0.1 mol dm^{-3} V_2O_5) at 450 °C equilibrated with ($P_{SO_2} + P_{SO_3}$ = 0.1 atm). P_{SO_2} = 1 atm (*a*), P_{SO_2}/P_{SO_3} = 9.74 (*b*), P_{SO_2}/P_{SO_3} = 3.60 (*c*), P_{SO_2}/P_{SO_3} = 0.58 (*d*), and P_{N_2} = 1 atm (*e*)

$^2E(d_{xz}, d_{yz})$, $^2B_2(d_{xy}) \longrightarrow {}^2B_1(d_{x^2-y^2})$ and $^2B_2(d_{xy}) \longrightarrow {}^2A_1(d_{z^2})$. For a configuration where the common C_{4v} symmetry of the distorted octahedron of the vanadyl complex is lowered, the double degeneracy of the first transition from the ground state is lost. Bands around 13 000 cm^{-1} are usually attributed to the first two transitions (allowing two for ^2E), while the other two transitions are commonly observed at *ca.* 16 000 cm^{-1} and above 25 000 cm^{-1}, respectively.[21] The band observed here at 13 700 cm^{-1} [probably due to the $^2B_2(d_{xy}) \longrightarrow {}^2E(d_{xz}, d_{yz})$ transition] is consistent with this. Based on 13 different spectra measured under pure SO_2 atmosphere in the temperature range 430–480 °C, the average experimental value for the molar absorption coefficient of the V^{IV} complexes at 730 nm, $\varepsilon_{V^{IV},730}$ was determined to be 18.91 ± 0.08 $dm^3\ mol^{-1}\ cm^{-1}$. This value generally compares well with molar absorption coefficients found for vanadyl complexes in water and other solvents.[21]

Spectrum (*e*) is obtained from a solution equilibrated with pure N_2 and exhibits only the tail of the charge-transfer band of a V^V complex, which has a very high intensity in the UV range of the spectrum.[4] Equilibrating the molten solution with pure O_2 or SO_3 led to measured absorbances at 730 nm that were identical within the experimental error, indicating that the same type of V^V complexes are formed in the solution. Slightly higher values were measured when N_2 was introduced, showing that the molten V_2O_5–$K_2S_2O_7$ mixture should be equilibrated with O_2 or SO_3 to stabilize vanadium in the +5 state. On the basis of 13 measured spectra at 450 °C the average experimental value for $\varepsilon_{V^V,730}$ was found to be 1.57 ± 0.02 $dm^3\ mol^{-1}\ cm^{-1}$. Furthermore, the values of $\varepsilon_{V^V,730}$ showed a small systematic variation with temperature, which can be represented by equation (2) for 430 < *T* < 480 °C (error 0.02 $dm^3\ mol^{-1}\ cm^{-1}$).

$$\varepsilon_{V^V,730} = -2.70 + 9.48 \times 10^{-3}\ T \qquad (2)$$

Redox equilibria of vanadium complexes. Fig. 3 [spectra (*b*)–(*d*)] shows that the 730 nm visible band due to the V^{IV} complexes becomes progressively stronger with increasing values of P_{SO_2}/P_{SO_3}. This seems to be due to the increased reduction of V^V to V^{IV}, caused by higher SO_2 partial pressures. For comparison a similar series of spectra is shown in Fig. 4. This series was also obtained at 450 °C for a 0.1 mol dm^{-3} V_2O_5 solution in the analogous mixed-cation molten $M_2S_2O_7$–V_2O_5 (M = 80% K + 20% Na) system, but using a closed cuvette (work in progress) in a wider wavelength range (using a Cary 14R spectrophotometer) and with spectrophotometric detection of SO_2 by a connected gas cuvette. This mixed-cation–solvent system reflects closely the promoter composition of a widely used industrial catalyst for sulfuric acid production.[8] However, in this series only the partial pressure of SO_2 was controlled, while the partial pressure of SO_3 was unknown, but presumably constant, *i.e.* equal to the unknown equilibrium partial pressure of SO_3 over the $M_2S_2O_7$ (M = 80% K + 20% Na) melt at 450 °C. The spectra of the two series (Figs. 3 and 4) are very similar, both showing an isosbestic point at ≈615 nm and a value close to 15 $dm^3\ mol^{-1}\ cm^{-1}$ for the molar absorption coefficient. Thus, the equilibrium (3)

$$a(V^V)_m(l) + SO_2(g) \rightleftharpoons b(V^{IV})_n(l) + SO_3(g) \qquad (3)$$

involving only two absorbing species, *i.e.* a V^V and a V^{IV} complex fits the experimental observations and justifies the application of equation (1) for the following calculations.

In such dilute molten solutions, previous investigations[4–7] suggest that V^V is present in the form of monomeric or dimeric complexes and V^{IV} presumably behaves in a similar way. The possible combinations of these proposed complexes give four simplified model equilibria, taking into account the two-electron transfer involved in the oxidation from S^{IV} to S^{VI}. Model 1, represented by equilibrium (4), gives rise to equation (5), which can also be written in the form of equation (6).

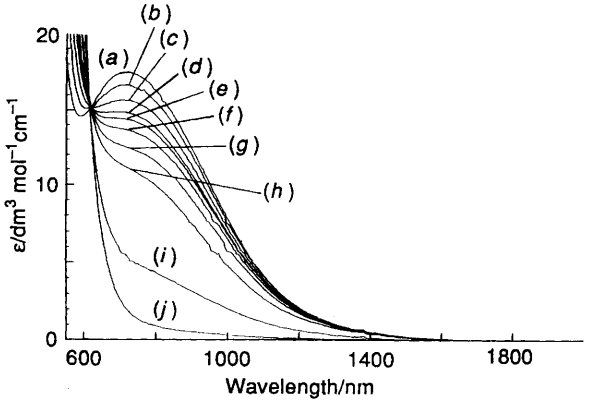

Fig. 4 VIS/NIR spectra of the mixture V_2O_5–$M_2S_2O_7$ (M = 80% K + 20% Na) at 450 °C equilibrated under partial P_{SO_2} = 0.1750 (*a*), 0.1000 (*b*), 0.0470 (*c*), 0.0257 (*d*), 0.0152 (*e*), 0.0100 (*f*), 0.0044 (*g*), 0.0087 (*h*), 0.0014 (*i*), and 0 atm (1 atm O_2) (*j*)

Similarly models 2–4, represented by equilibria (7), (10) and (13), respectively, give rise to the corresponding equations (8) and (9), (11) and (12), and (14) and (15).

$$(V^V)_2 + SO_2 \rightleftharpoons (V^{IV})_2 + SO_3 \qquad (4)$$

$$K_1 = \frac{\frac{1}{2}[V^{IV}]}{\frac{1}{2}[V^V]} \frac{P_{SO_3}}{P_{SO_2}} \qquad (5)$$

$$\frac{[V^{IV}]}{[V^V]} = K_1 \times \frac{P_{SO_2}}{P_{SO_3}} \qquad (6)$$

$$(V^V)_2 + SO_2 \rightleftharpoons 2(V^{IV}) + SO_3 \qquad (7)$$

$$K_2 = \frac{[V^{IV}]^2}{\frac{1}{2}[V^V]} \times \frac{P_{SO_3}}{P_{SO_2}} \qquad (8)$$

$$\frac{2[V^{IV}]^2}{[V^V]} = K_2 \frac{P_{SO_2}}{P_{SO_3}} \qquad (9)$$

$$2(V^V) + SO_2 \rightleftharpoons 2(V^{IV}) + SO_3 \qquad (10)$$

$$K_3 = \frac{[V^{IV}]^2}{[V^V]^2} \times \frac{P_{SO_3}}{P_{SO_2}} \qquad (11)$$

$$\frac{[V^{IV}]^2}{[V^V]^2} = K_3 \frac{P_{SO_2}}{P_{SO_3}} \qquad (12)$$

$$2(V^V) + SO_2 \rightleftharpoons (V^{IV})_2 + SO_3 \qquad (13)$$

$$K_4 = \frac{\frac{1}{2}[V^{IV}]}{[V^V]^2} \times \frac{P_{SO_3}}{P_{SO_2}} \qquad (14)$$

$$\frac{[V^{IV}]}{2[V^V]^2} = K_4 \frac{P_{SO_2}}{P_{SO_3}} \qquad (15)$$

By using equation (1) and the obtained $\varepsilon_{V^{IV}}$ and ε_{V^V} values (see above) $c_{V^{IV}}$ and c_{V^V} could be calculated and the concentration quotients for each model could be determined. Plots of these quotients *vs.* P_{SO_2}/P_{SO_3} are shown in Fig. 5 for the 22 different measurements at 450 °C. It is evident that for a correct model a linear plot should be observed with a slope corresponding to the equilibrium constant. From Fig. 5, models 2 and 3 give essentially linear plots, while models 1 and 4 give plots that deviate considerably from linearity.

Temperature dependence and enthalpy of redox equilibria. In Fig. 6 all data for models 2 and 3 obtained in the temperature

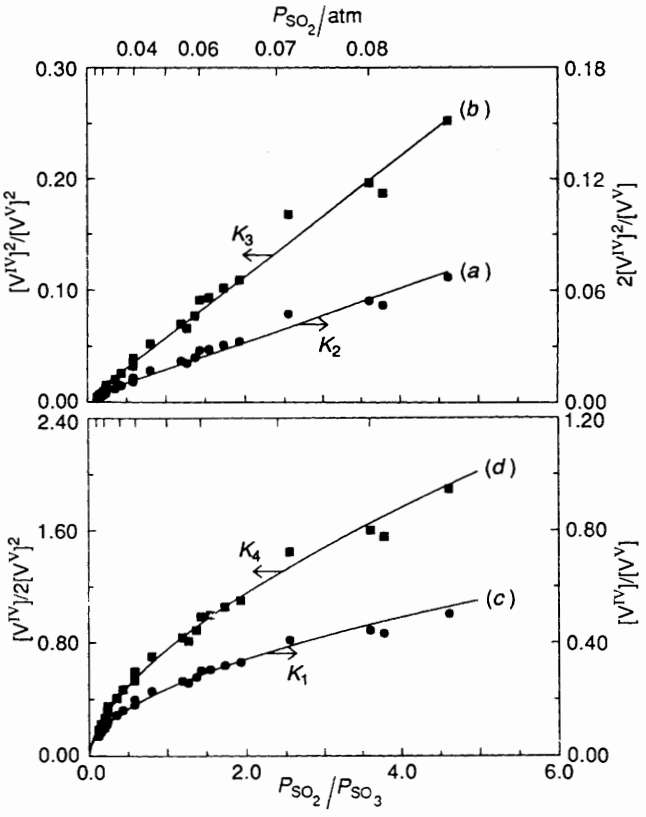

Fig. 5 Plots of concentration quotients for model 2 (*a*), model 3 (*b*), model 1 (*c*) and model 4 (*d*) *vs.* P_{SO_2}/P_{SO_3}. The data are obtained at 450 °C from a V_2O_5–$K_2S_2O_7$ mixture with $c_0 = 0.1$ mol dm^{-3} V_2O_5

range 430–480 °C are plotted and essentially linear dependencies are observed in all cases.

In addition a parametric analysis has been applied to the spectra for each of the four model equilibria giving the smallest deviation between the measured and calculated absorption (A/l) at 730 nm. By variation of the equilibrium constant, and $c_{V^{IV}}$ and c_{V^V}, the optimum value for $\varepsilon_{V^{IV},730}$ and the variance in the absorption coefficients could be calculated using equation (1) and these data have been deposited (SUP No. 57016). From this data models 1 and 4 could be excluded at all temperatures on a 95% significance level.

From the slopes of the plots in Fig. 6 the equilibrium constants for the two models were determined for each temperature and plotted as $\ln K$ *vs.* $1/T$ in Fig. 7. The expressions for the redox equilibria according to models 2 and 3 are deduced from previous knowledge of the complex chemistry of V^V in disulfate melts obtained in previous investigations[4–7,22] and adopting the V^{IV} configuration involving a VO^{2+} unit co-ordinated to two bidentate sulfate ligands as discussed above. The slopes of the plots shown in Fig. 7 correspond to the enthalpies, $\Delta H°$, for equilibria (16)

$$[(VO)_2O(SO_4)_4]^{4-}(l) + SO_2(g) \rightleftharpoons 2[VO(SO_4)_2]^{2-}(l) + SO_3(g) \quad (16)$$

for model 2 ($\Delta H° = -107 \pm 4$ kJ mol^{-1}) and (17), which can

$$2[VO_2(SO_4)]^-(l) + S_2O_7^{2-}(l) + SO_2(g) \rightleftharpoons 2[VO(SO_4)_2]^{2-}(l) + SO_3(g) \quad (17)$$

alternatively be formulated as in equilibrium (18) for model 3

$$2[VO_2(SO_4)(S_2O_7)]^{3-}(l) + SO_2(g) \rightleftharpoons 2[VO(SO_4)_2]^{2-}(l) + S_2O_7^{2-}(l) + SO_3(g) \quad (18)$$

($\Delta H° = -122 \pm 2$ kJ mol^{-1}).

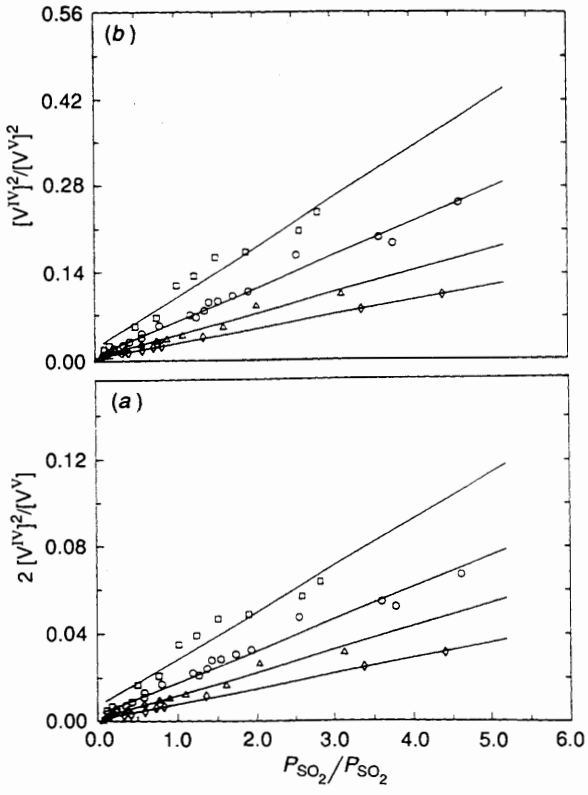

Fig. 6 Plots of concentration quotients for models 2 (*a*) and 3 (*b*) *vs.* P_{SO_2}/P_{SO_3} at 435 (□), 450 (○), 465 (△) and 480 °C (◇). The data are obtained from a V_2O_5–$K_2S_2O_7$ mixture with $c_0 = 0.1$ mol dm^{-3} V_2O_5

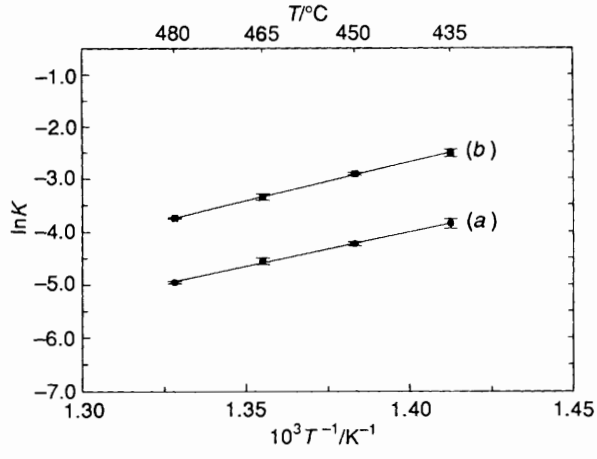

Fig. 7 Plots of $\ln K$ *vs.* $1/T$ for models 2 (*a*) and 3 (*b*). The concentration of $S_2O_7^{2-}$ has not been taken into account for the calculation of K_3 (see text)

It has previously[4] appeared to be impossible to distinguish between the two monomeric V^V complexes participating in the redox equilibria (17) and (18). It should be pointed out that the concentration of $S_2O_7^{2-}$ has not been considered for the calculation of K_3. However, in 0.1 mol dm^{-3} V_2O_5 solutions in $K_2S_2O_7$, $[S_2O_7^{2-}] = 8.120$ mol dm^{-3} at 450 °C, as calculated from the densities of the V_2O_5–$K_2S_2O_7$ system obtained previously.[6] In the temperature range 435–480 °C investigated here, $[S_2O_7^{2-}]$ varies by less than 1% from this value and accordingly it can be considered constant. Therefore the slope of the plot for model 3 in Fig. 7, and the enthalpy, $\Delta H°$, are not affected. It is noteworthy that previous cryoscopic measurements[4] show that V^V is most probably present as a monomeric complex in the concentration range of the present investigation. Thus, model 3 is favoured.

On increasing c_0 an increase in the molar absorption coefficient, reflecting an increased degree of vanadium reduction, $c_{V^{IV}}/c_0$, is observed. Thus for example at 450 °C and with $P_{SO_2} = 0.06$ atm (*i.e.* $P_{SO_3} = 0.04$ atm), values of $c_{V^{IV}}/c_0 = 0.23$, 0.35 and 0.55 are obtained for melts with $c_0 = 0.1$, 0.25 and 0.5 mol dm^{-3} V_2O_5, respectively.

Plots of the concentration quotients *vs.* P_{SO_2}/P_{SO_3} for melts with $c_0 = 0.25$ mol dm^{-3} V_2O_5 (based on 17 different spectra) also show a better fit to a straight line for models 2 and 3 than for models 1 and 4. This provides further evidence for the presence of monomeric V^{IV} complexes showing that no dimerization (or polymerization) has occurred.

It is not possible to exclude models 1 and 4 in the most concentrated melt, *i.e.* $c_0 = 0.5$ mol dm^{-3} V_2O_5, as the plots of the concentration quotients *vs.* P_{SO_2}/P_{SO_3} (based on 10 different spectra) show little deviation from linearity. This might be due to a gradual polymerization, which probably occurs progressively with increasing vanadium concentration.

ESR Measurements.—The complex formation of V^{IV} can be studied exclusively by ESR since V^{IV} is paramagnetic having a $3d^1$ electronic configuration, while V^V is diamagnetic with a $3d^0$ configuration in the ground state. The nuclear spin of ^{51}V, which is the predominant isotope of naturally abundant vanadium, is $+\frac{7}{2}$. Therefore, solutions of monomeric V^{IV} complexes give rise to characteristic eight-line spectra with a g value of *ca.* 1.97 and a hyperfine coupling constant, $\bar{A}$, of *ca.* 100 G due to the coupling between the electron and the vanadium nucleus.[23]

The ESR spectra obtained at 450 °C for 0.1, 0.25 and 0.5 mol dm^{-3} solutions of V_2O_5 in $K_2S_2O_7$ under various partial pressure ratios, P_{SO_2}/P_{SO_3} exhibit a characteristic eight line spectral feature, with $g = 1.979 \pm 0.005$ and $\bar{A} = 111 \pm 5$ G. The hyperfine coupling constant is considerably larger, by *ca.* 20 G, than expected[23] for vanadyl complexes with a similar g value. For dimeric or polymeric V^{IV} complexes the electron couples with two or more nuclei, giving rise to complicated unresolved multiline spectra with a very large line width, very different from the spectra of monomeric V^{IV} complexes.[24–26] Furthermore only dimers with a metal–metal bond are expected to have all-paired electrons and to be ESR silent. Such complexes are very unlikely in the solutions studied here since all structures of V^{III}, V^{IV} and V^V salts isolated until now[12–16,22] exhibit sulfate or oxide bridging of the vanadium atoms, and all of the V^{IV} complex compounds isolated to date are ESR active.[17,27] Thus only monomeric V^{IV} seems to be present in the molten mixtures analogous to those investigated by UV/VIS spectrophotometry. This gives further support to model 2 or 3, while models 1 and 4 can be ruled out since they involve dimeric V^{IV} complexes.

In order to examine the possible influence of the temperature on V^{IV} complex formation, the temperature dependence of the ESR spectra of 0.25 mol dm^{-3} V_2O_5 in $K_2S_2O_7$ has been studied in the range 355–478 °C. Fig. 8 shows the temperature dependence at a fixed ratio $P_{SO_2}/P_{SO_3} = 3.8$ and at $P_{SO_2} + P_{SO_3} = 1$ atm. By lowering the temperature gradually from 478 to 378 °C a continuous increase of the signal intensity, and thereby of the V^{IV} concentration, is observed. This is in accordance with the results of the spectrophotometric measurements, where the redox equilibria proposed are shifted towards V^{IV} by lowering the temperature. The g and $\bar{A}$ values of the eight-line spectra do not change (within the experimental error) by cooling to 378 °C, showing that the same monomeric V^{IV} complex is present at all temperatures. By further lowering the temperature to 355 °C, a sharp, slightly anisotropic, line with $g_{iso} = 1.963 \pm 0.005$ and $\Delta H = 94 \pm 5$ G dominates the spectrum at the expense of the eight-line feature due to the monomeric V^{IV} complex which however is still visible. This is in agreement with a previous ESR investigation of an industrial catalyst,[17] where the precipitation of the V^{IV} compound $K_4(VO)_3(SO_4)_5$ gave rise to a sharp central line in the spectrum

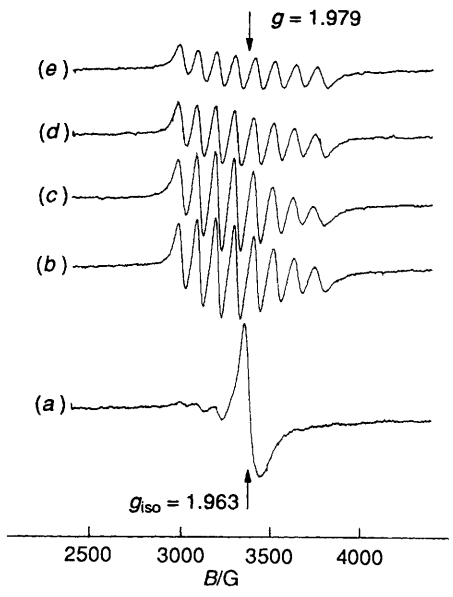

Fig. 8 Temperature dependence of the ESR spectra of V_2O_5–$K_2S_2O_7$ melts ($c_0 = 0.25$ mol dm^{-3} V_2O_5). $P_{SO_2}/P_{SO_3} = 3.8$ and $P_{SO_2} + P_{SO_3} = 1$ atm: $T = 355$ (*a*), 378 (*b*), 401 (*c*), 431 (*d*) and 478 °C (*e*)

($g_{iso} = 1.967 \pm 0.002$ and $\Delta H = 72 \pm 2$ G). As judged from the spectral features, the V^{IV} compound precipitating in the present investigation is probably not $K_4(VO)_3(SO_4)_5$ or $VOSO_4$, which has a very different anisotropic spectrum.[27] Probably the compound is very similar to $K_4(VO)_3(SO_4)_5$, *i.e.* corresponding to another stoichiometric combination of K_2SO_4 and $VOSO_4$. The formation of different compounds is most probably due to the large differences in the concentration (0.25 mol dm^{-3} V_2O_5 in the present investigation compared to ~2 mol dm^{-3} V_2O_5 in the industrial catalyst) and also in the gas composition (SO_2, 79 and SO_3, 21% *vs.* SO_2, 10; O_2, 11 and N_2 79%).[11,17]

A quantitative examination of the spectra in Fig. 8 (double integration of the spectra of the dissolved V^{IV} at 401 °C and of the precipitated V^{IV} at 355 °C) shows that only *ca.* 30% of the dissolved V^{IV} is found in the precipitate. This might be due to formation of ESR silent V^{III} compounds that are known to precipitate in melts which are relatively dilute in vanadium upon lowering the temperature.[11] The attempted isolation of these V^{III} compounds will be the subject of future investigations.

Acknowledgements

This work has been supported by the EEC BRITE-EURAM II (contract no. BRE2.CT93.0447) and Human Capital and Mobility (contract no. ERBCHBG. CT92.0129) Programmes. Support from the Danish Natural Science Research Council and the General Secretariat of Research and Technology of the Greek Ministry of Industry and Energy is gratefully acknowledged. A. Zissios (Institute of Chemical Engineering and High Temperature Chemical Processes) and K. W. Pedersen (Technical University of Denmark) are thanked for experimental assistance. The authors are indebted to Professor G. N. Papatheodorou for helpful discussions and valuable comments.

References

1 P. Mars and J. G. H. Maessen, *J. Catal.*, 1968, **10**, 1.
2 G. K. Boreskov, G. M. Polyakova, A. A. Ivanov and V. M. Mastikhin, *Dokl. Akad. Nauk. SSSR*, 1973, **210**, 626.

3 J. Villadsen and H. Livbjerg, *Catal. Rev. Sci. Eng.*, 1978, **17**, 203.
4 N. H. Hansen, R. Fehrmann and N. J. Bjerrum, *Inorg. Chem.*, 1982, **21**, 744.
5 R. Fehrmann, M. Gaune-Escard and N. J. Bjerrum, *Inorg. Chem.*, 1986, **25**, 1132.
6 G. Hatem, R. Fehrmann, M. Gaune-Escard and N. J. Bjerrum, *J. Phys. Chem.*, 1987, **91**, 195.
7 G. E. Folkmann, G. Hatem, R. Fehrmann, M. Gaune-Escard and N. J. Bjerrum, *Inorg. Chem.*, 1993, **32**, 1559.
8 D. A. Karydis, S. Boghosian and R. Fehrmann, *J. Catal.*, 1994, **145**, 312.
9 V. Bandur, K. M. Eriksen, G. E. Folkmann, G. Hatem, R. Fehrmann and N. J. Bjerrum, unpublished work.
10 G. E. Folkmann, G. Hatem, R. Fehrmann, M. Gaune-Escard and N. J. Bjerrum, *Inorg. Chem.*, 1991, **30**, 4057.
11 S. Boghosian, R. Fehrmann, N. J. Bjerrum and G. N. Papatheodorou, *J. Catal.*, 1989, **119**, 121.
12 R. Fehrmann, S. Boghosian, G. N. Papatheodorou, K. Nielsen, R. W. Berg and N. J. Bjerrum, *Inorg. Chem.*, 1989, **28**, 1847.
13 R. Fehrmann, S. Boghosian, G. N. Papatheodorou, K. Nielsen, R. W. Berg and N. J. Bjerrum, *Inorg. Chem.*, 1990, **29**, 3294.
14 R. Fehrmann, B. Krebs, G. N. Papatheodorou, R. W. Berg and N. J. Bjerrum, *Inorg. Chem.*, 1986, **25**, 1571.
15 R. Fehrmann, S. Boghosian, G. N. Papatheodorou, K. Nielsen, R. W. Berg and N. J. Bjerrum, *Acta Chem. Scand.*, 1991, **45**, 961.
16 R. W. Berg, S. Boghosian, N. J. Bjerrum, R. Fehrmann, B. Krebs, N. Strater, O. S. Mortensen and G. N. Papatheodorou, *Inorg. Chem.*, 1993, **32**, 4714.
17 K. M. Eriksen, R. Fehrmann and N. J. Bjerrum, *J. Catal.*, 1991, **132**, 263.
18 A. Durand, G. Picard and J. Vedel, *J. Electroanal. Chem. Interfacial Electrochem.*, 1981, **127**, 169.
19 V. M. Mastikhin, G. M. Polyakova, Y. Zyulkovskii and G. K. Boreskov, *Kinet. Katal.*, 1970, **11**, 1463; *Kinet. Catal. (Engl. Transl.)*, 1970, **11**, 1219.
20 C. J. Balhausen and H. B. Gray, *Inorg. Chem.*, 1962, **1**, 111.
21 J. Selbin, *Coord. Chem. Rev.*, 1966, **1**, 293.
22 K. Nielsen, R. Fehrmann, K. M. Eriksen, *Inorg. Chem.*, 1993, **32**, 4825.
23 M. C. R. Symons, *Chemical and Biochemical Aspects of Electron Spin Resonance Spectroscopy*, Van Nostrand Reinhold, Wokingham, 1978.
24 R. L. Belford, N. D. Chasteen, H. So and R. E. Tapscott, *J. Am. Chem. Soc.*, 1969, **91**, 4675.
25 H. Toftlund, S. Larsen and K. S. Murray, *Inorg. Chem.*, 1991, **30**, 3964.
26 L. C. Dickinson, R. H. Dunhill and M. C. R. Symons, *J. Chem. Soc., A*, 1970, 922.
27 K. M. Eriksen, Ph.D. Thesis, Technical University of Denmark, 1993.

Received 30*th December* 1993; *Paper* 3/07584B